JCZ: Zoologischer Anzeiger - A Journal of Comparative Zoology 304 (2023) 10–20

Contents lists available at ScienceDirect

Zoologischer Anzeiger

journal homepage: www.elsevier.com/locate/jcz

Ultrastructural characterization of the putative defensive glands (warts) in the sessile, colonial rotifer *Sinantherina socialis* (Gnesiotrocha; Floscullariidae)

Robert L. Wallace [a], Katrina M. Dash [b], Thiago Q. Araújo [c], Elizabeth J. Walsh [d], Siddhartha Das [d], Rick Hochberg [c,*]

[a] *Ripon College, Ripon, WI, 54971, USA*
[b] *Eastern Virginia Medical School, Norfolk, VA, 23501, USA*
[c] *University of Massachusetts Lowell, Lowell, MA, 01854, USA*
[d] *University of Texas at El Paso, El Paso, TX, 79968, USA*

ARTICLE INFO

Handling Editor: Maikon Di Domenico

Keywords:
Defense
Freshwater
Invertebrate
Predator
Prey
Unpalatable

ABSTRACT

Female *Sinantherina socialis* are freshwater, sessile, colonial rotifers that possess two pairs of distinctive glands (warts) located below the corona. Previous studies demonstrated that colonies are unpalatable to many invertebrate and vertebrate predators; those authors suggested that the warts were a possible source of a chemical deterrent to predation. Here we explore wart ultrastructure and cytochemisty to determine whether the warts function as exocrine glands and if their contents display any allomone-like chemistry, respectively. Externally, the warts appear as elevated bulges without pores. Internally, the warts are specialized regions of the integumental syncytium and therefore acellular. The lipid stain Nile Red labels all four warts. Two lipid membrane probes (sphingomyelin and phosphatidylinositol) also bind the warts and may be staining internal secretion vesicle membranes. In fact, wart ultrastructure is defined by hundreds of membrane-bound secretion vesicles packed tightly together. The vesicles are mostly electron-lucent and crowded into a well-defined cytoplasmic space. The cytoplasm also contains abundant ribosomes, rough endoplasmic reticulum, mitochondria, and Golgi, but nuclei are generally positioned peripheral to the packed vesicles. Absence of muscles around the warts or any signs of direct innervation suggests expulsion of gland contents is forced by general body contraction. A single specimen with 'empty' warts implies that secretions are released en masse from all glands simultaneously. The identity of the chemical secretion remains to be determined, but the lack of osmium and uranyl acetate staining suggests a low abundance or absence of phenols, unsaturated lipids, or NH_2 and –COOH groups. This absence, combined with the positive Nile Red staining, is interpreted as evidence that vesicles contain saturated fatty acids such as lactones that are unpalatable to predators.

1. Introduction

Rotifera (*sensu stricto*) is a small phylum (~2000 species) of microscopic aquatic metazoans (~40–2000 μm) that are found wherever liquid water is present for even a few days (Walsh et al., 2014). While a few species are found in saline systems (Fontaneto et al., 2008; Fontaneto et al., 2006; Fradkin, 2001; Walsh et al., 2008), most rotifers are present in freshwaters, including lakes, ponds, roadside ditches, rock pools, and cryoconite holes on glaciers, as well as the water film covering terrestrial mosses (Wallace et al., 2015; Walsh et al., 2014). Due to their small size, rotifers fall prey to a variety of predators including ciliates (Buonanno et al., 2017; Buonanno et al., 2020; Buonanno et al., 2013), cladocerans (Herzog et al., 2016; Stenson, 1987), copepods (Almeda et al., 2017; Buskey et al., 2017), insects and mites (Hampton and Gilbert, 2001; Hershey and Dodson, 1987; Kerfoot, 1982; Kerfoot et al., 1980; Walsh et al., 2006), hydra (Walsh et al., 2006), and gastrotrichs (Balsamo et al., 2020). Aquaculturists have taken advantage of their size and nutritional value to culture various species that they feed to commercially important hatchling fish and the larval stages of invertebrates, as well as adult fish with small mouths (Allen et al., 2016;

* Corresponding author.
E-mail address: Rick_hochberg@uml.edu (R. Hochberg).

https://doi.org/10.1016/j.jcz.2023.03.001
Received 30 January 2023; Received in revised form 5 March 2023; Accepted 8 March 2023
Available online 16 March 2023

Lubzens et al., 1989; Snell et al., 2018; Wallace et al., 2006).

Their small size allows some rotifers to evade certain predators. Thus, it is curious that some species form colonies given that the larger size of colonies should increase risk of predation by visual predators (Wallace 1987). However, that risk may be reduced in many species by morphological adaptations that allow them to avoid predation. These adaptations include spines, the ability to make rapid jumps, and gelatinous sheaths (Gilbert 1980; Wallace et al., 2006; Wallace et al., 2015). For example, individuals in the planktonic species *Sinantherina spinosa* (Thorpe, 1893) possess short spines on their anteroventral surface; when the colony is disturbed all the individuals bend dorsally thereby collectively exposing the spines to the margin of the colony. These spines may deter predation from predators that attempt to swallow the colony whole by irritating sensitive tissues in their buccal cavities (Thorpe, 1893; Wallace et al., 2015). Additionally, three other species of *Sinantherina* — *Sinantherina procera* (Thorpe, 1893), *Sinantherina semibullata* (Thorpe, 1889), and *Sinantherina socialis* (Linnaeus, 1758) — possess protuberances (warts) on their anteroventral surface near the corona; these have been posited to be glandular and possess biochemical defensive qualities (Felix et al., 1995; Hochberg et al., 2015). Indeed, experiments on palatability of *S. socialis* colonies revealed that many vertebrate and invertebrate predators actively reject them once captured (Felix et al., 1995; Walsh et al., 2006). Snell (1998) reported that the unpalatability factor could be transferred to a food comprising freeze-dried tubifex worms that had been rehydrated in a crude homogenate of *S. socialis* colonies. To date, we know nothing of the structure of the warts or of their chemical constituents. A previous study using scanning electron microscopy showed that the integument covering and surrounding the warts were identical to the rest of the body, and there was no evidence of pores in the integument that might suggest a site of chemical release (Hochberg et al., 2015).

In this study, we explore the cytochemistry and ultrastructure of the warts in *S. socialis* to answer three questions. (1) Are the warts glandular? (2) Do they exhibit evidence of exocrine secretion? (3) Can we characterize their secretion contents? To address these questions, we use fluorescent probes and confocal laser scanning microscopy (CLSM) to describe their contents and determine whether the warts are innervated or supplied with muscles. We also used scanning electron (SEM) and transmission electron microscopy (TEM) to characterize their external and internal structure.

2. Methods

2.1. Collection and processing for confocal laser scanning microscopy

Cultures of *S. socialis* used for cytochemical staining of the warts were started from specimens collected as whole colonies from two sites: (1) Tule Cattle Tank at Big Bend National Park, Texas, USA (29.2420833, −103.4425; 914 m); (2) Rio Grande near El Paso, Texas, USA (31.886086, −106.598892; 1144 m). For controls we used three, non-colonial, free-swimming species known to be palatable to a variety of freshwater predators. (1) Cultures of *Euchlanis dilatata* Ehrenberg, 1830 were originally isolated from the Rio Grande near El Paso (see above). (2) Cultures of *Epiphanes hawaiiensis* Schröder & Walsh, 2007 were started from specimens isolated from Lake Waia, Hawaii (19.811152, −155.477479; 3892 m). (3) *Epiphanes chihuahuaensis* Schröder & Walsh, 2007 were collected from Hueco Tanks State Park and Historic Site (31.923425, −106.042257).

Three types of stains were used to investigate the chemistry of the warts of *S. socialis,* as well as the two species used for controls. To localize proteins, we used LavaCellTM (Active Motif North America, Carlsbad, CA, USA), a water-soluble stain that fluoresces at 610 nm when excited at 405, 488, or 532 nm (Active Motif, Carlsbad, CA). Preserved rotifers were stained for 30 min, following manufacturer instructions (Active Motif, Carlsbad, CA). To localize neutral lipids, we used Nile Red (Life Technologies; Thermo Fisher, Carlsbad, CA), a dye that emits at ~590 nm when excited at ca. 515–560 nm (Greenspan et al., 1985). Following techniques used by Sonda et al. (2008) for the protozoan parasite *Giardia lamblia* (Lambl, 1859), we stained preserved rotifers in small glass wells for 20 min. Additionally, to ascertain whether the warts of *S. socialis* were degraded by fixatives, we stained live rotifers with Nile Red for 15 min at room temperature, following techniques used by Carman et al. (1991) for copepods. We also used fluorescent Bodipy or NBD (nitrobenzoxadiazole)-conjugated lipid probes such as phosphatidylcholine (PC), phosphatidylglycerol (PG), phosphatidylinositol (PI), and sphingomyelin (SM) (Life Technologies, Thermo Fisher, Carlsbad, CA (Stevens et al., 1997). Rotifers were incubated with these probes at 37 °C for 30 min (or as otherwise specified), anesthetized in carbonated water, washed twice in phosphate-buffered saline (1X PBS), and fixed in 4% methanol-free paraformaldehyde. Slides were thoroughly rinsed three times in PBS, cover slips were mounted using DAKO mounting media (DAKO Corp., Carpinteria, CA), and specimens examined using a Zeiss LSM5 PASCAL confocal laser scanning microscope. Luminescence of the images was quantified in *ImageJ* (Schneider et al., 2012).

Colonies of *S. socialis* were stained for muscles and neurites to determine whether the glands were muscular and controlled by neural stimulation. Colonies were removed from submerged hydrophytes (*Utricularia* spp.) in Mascuppic Lake (42.6783333, −71.4006333333; 58 m) and Locust Pond (42.686175, −71.4393861111; 53 m) in Tyngsborough, Massachusetts (USA). Colonies were isolated in 50 ml bowls of source water and photographed with a Zeiss Stemi stereomicroscope® and Sony Handycam® digital camera. Some colonies were transferred to small bowls of water (5 ml) and anesthetized with the addition of 1–2 mls of commercially available carbonated water. After anesthetization (~2–3 min), portions of colonies were transferred to glass slides, compressed with a coverslip, and photographed using a Zeiss Axioskop® equipped with a Sony Handycam digital camera. Colonies were then preserved in 4% paraformaldehyde in 0.1 M phosphate buffer saline (pH 7.4) for 24 h at 5 °C. Colonies were dissected to free individual specimens and then placed in buffer for 2 h prior to transfer into a solution of buffer plus 0.5% Triton X-100 (PBT) for 2 h. A total of eight animals were prepared for staining: three were omitted from primary antibodies and used as negative controls, and five were placed in a blocking solution consisting of 1% bovine serum albumin (Sigma–Aldrich) and 0.1 M PBS overnight. Animals were then rinsed in 0.1 M PBS for 2 h and transferred into a primary antibody solution of Rabbit anti-5HT (1:2000, N = 6, Sigma–Aldrich)) for 24 h at 5 °C on a rotator. Animals were next were rinsed in 0.5% PBT for 24 h and incubated in secondary antibody solution (goat anti-rabbit IgG 546 (1:200, Sigma–Aldrich)) for 24 h at 5 °C on a rotator. Following the secondary solution, specimens were rinsed in 0.5% PBT for 24 h and incubated in Alexa-488 phalloidin (Invitrogen) for 1–2 h prior to mounting in Fluoromount G (Electron Microscopy Sciences, Hatfield PA).

Specimens were examined on a Leica TCS SP8 LSCM microscope at the University of Massachusetts, Lowell. Leica Application Suite X (LAS X) was used to collect a series of optical sections at 0.05–0.1 μm/slice, processed as z-stacks, and saved as LIF files. Files were analyzed in Imaris x64 (v. 9.9.0) to render 3D images, analyze each single stack, and create JPEGs. No manipulations of the images were made other than changes of color (false coloring or grayscale) or cropping.

2.2. Processing for electron microscopy

Colonies and individual specimens from Massachusetts were preserved in 2.5% glutaraldehyde in 0.1 M sodium cacodylate buffer with sucrose for 1 h (4 × 15 min) at room temperature (RT). These specimens were then post fixed in 1% OsO_4 in 0.1 M sodium cacodylate buffer for 1 h at RT and rinsed again in buffer (4 × 15 min) at RT. Animals were then transferred through an ethanol series (50, 70, 90, and 100%; 2x) at 15 min each in a separate glass bowl (5 ml). For scanning electron microscopy, several colonies were transferred into 60 μm mesh screen-covered

BEEM® capsules (Electron Microscopy Sciences, PA, USA) and critically point dried in a Tousimis SAMDRI-795® using liquid CO_2. Animals were then placed on carbon, tape-coated aluminum SEM stubs and coated in gold using a Denton Vacuum Desk IV® sputter coater. These specimens were finally examined on a JEOL JSM 6390® SEM in the Materials Characterization Laboratory at the University of Massachusetts Lowell (MA, USA).

For transmission electron microscopy, five specimens were removed from two adult colonies, placed in 100% ethanol, and transferred through two changes (2 h each) of a 1:1 and 3:1 mixture of ethanol: Dr. Spurr's low viscosity resin (Electron Microscopy Sciences, Hatfield, PA, USA) in microcentrifuge tubes on a rotator. The specimens were then transferred to pure resin and rotated overnight at RT before being transferred to individual BEEM capsules and cured in an oven at 68 °C for 24 h. Resin blocks were trimmed and cut on a Leica UC7® ultramicrotome using glass knives to produce silver sections. These were collected on copper grids and stained in uranyl acetate (2 min) and lead citrate (2 min). Sections were then examined on a Philips CM10® at 80 KHz and equipped with a side-mounted Gatan Orius® digital camera. Measurements of organelles were taken using Fiji (*ImageJ*, v2.1.0/1.53c) (Schneider et al., 2012). Digital photographs were cropped using Adobe Photoshop® (Release 22.5, 1990–2021); no additional changes were made to the photographs.

3. Results

3.1. Light microscope observations

The warts of *S. socialis* appear as white spots under the reflected light of a stereomicroscope (Fig. 1A–C), but they may appear translucent with the transmitted light of a compound microscope (Fig. 1D and E) or even appear as dark spots under the incident light of a compound microscope (Fig. 4A). Specimens preserved in glutaraldehyde and/or OsO_4 and viewed with brightfield microscopy may show a slight darkening of the warts, but they remain mostly translucent and not obviously stained (Fig. 1D and E, 4).

3.2. Confocal observations of probes to determine wart chemistry

Staining with LavaCell revealed widespread fluorescence in the muscles and body wall. The warts did not show unusually high concentrations of fluorescence (see Supplemental Document Fig. 1).

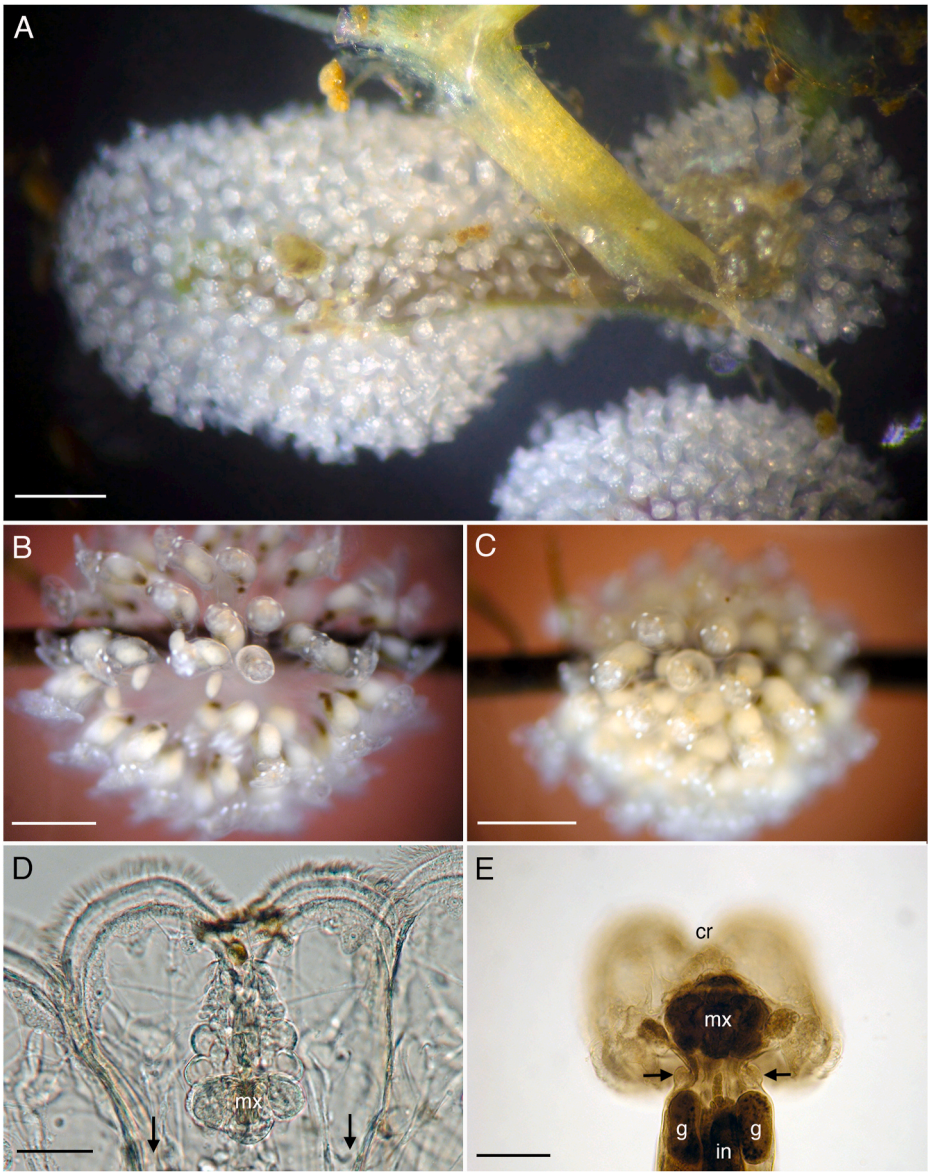

Fig. 1. Female *Sinantherina socialis* visualized with light microscopy. A) Three asexual female colonies on a submerged hydrophyte; B) Closeup of a small asexual colony (~40–50 individuals) with their coronae extended to feed. Small white dots are the warts; C) Same colony as in C but after a disturbance: their coronae have retracted, exposing more prominently the four warts on each individual; D) Closeup of coronal region of an osmium tetroxide-fixed specimen. Black arrows point to the warts, which are translucent in this preparation; E) Specimen fixed in glutaraldehyde, postfixed in OsO_4, and embedded in resin. Black arrows point to translucent warts. Abbreviations: cr, corona; g, gastric glands; in, intestine, mx, mastax. Scale bars: A, 1000 μm. B, 500 μm. C, 500 μm. D, 15 μm. E, 20 μm.

Staining with Nile Red showed strong fluorescence in the gut, developing embryos, and warts (Fig. 2B; Supplemental Document): the intensity of the staining in the warts made it difficult to determine where the lipids were concentrated, i.e., in the vesicles or elsewhere in the wart bodies (Supplemental Document Fig. 1). In *E. dilatata* and *E. hawaiiensis*, the distribution of lipids showed no remarkable pattern as was observed in *S. socialis* (Fig. 2E). Of the four lipids (PC, PG, PI, and SM), only phosphatidylinositol (PI) and sphingomyelin (SM) showed substantial staining in the warts (Fig. 2C). According to the *ImageJ* analysis, SM had the strongest reaction, with a luminescence ratio of ~2:1 compared to other lipids.

3.3. Confocal observations of muscles and nerves

We used CLSM to view the region around the corona to determine whether there were any muscles or neurites that supplied the warts (Fig. 3). Earlier observations suggested no such evidence (Hochberg and Lilley, 2010), but these observations were based on epifluorescence microscopy that lacked the magnification and resolution of CLSM. Current observations did not reveal any neurites (containing alpha tubulin, serotonin, or FMRFamide) innervating the warts (Fig. 3A and B). All three antibody stains showed fluorescence in similar regions. No muscles or actin-rich cells supplied warts, though several longitudinal muscles were proximal to the warts (Fig. 3C).

3.4. Ultrastructural observations

Several specimens were examined with transmission electron microscopy, but in only one specimen could all four warts be identified (in separate sections). In this specimen, and six of the other adult specimens (n = 7 total processed), the warts appeared similar in ultrastructure and always distinguishable from the general integument. The size of the warts and their shapes differed due to plane of section, but there did appear to be some shrinkage based on a size and shape comparison to live and preserved wholemount specimens. Regardless of shrinkage, their internal features were all largely identical (Fig. 4C–F). The rest of the body integument has been described previously (Hochberg et al., 2015).

All warts appeared as swellings due to the collection of numerous membrane-bound vesicles and other organelles accumulating in the cytoplasm of the integument (Figs. 4 and 5). Like the integument that surrounds the rest of the body (Hochberg et al., 2015), the outer layer of integument in the warts is an electron-dense zone called the intracytoplasmic lamina (ICL), which is covered by an apical plasma membrane (Fig. 5). The ICL is wavy in appearance due to the longitudinal ridges that traverse the integument (Figs. 4 and 5; Hochberg et al., 2015). The ICL had an average thickness of 218 nm (SD = 17.7 nm; n = 35 sections), which was similar to the rest of the integument on other portions of the body. The ICL had a somewhat cloudy but fibrous appearance (Fig. 5E and F). The fibers appeared to form a sort of meshwork and they did not extend in any obvious orientation or direction (relative to the a:p axis).

Beneath the ICL was a swollen region of cytoplasm that contained membrane-bound vesicles, abundant ribosomes, Golgi, rough endoplasmic reticulum (rER), mitochondria, some autophagic bodies, and a single nucleus (Figs. 3–6). The nucleus was not always visible in sections, but when present, was generally positioned to the side of the swollen region and never directly among the vesicles (exception noted below). The cytoplasm was largely dominated by secretion vesicles that created the swollen appearance of the warts; warts were elevated 6.0–9.9 μm above the remaining integument (not including the wavy ridges; Fig. 4). Membrane-bound vesicles were generally oval to round and ranged in size from 149 to 201 nm diameter ($\bar{x}$ = 175.5 nm; SD = 17.7 nm; n = 40 from four specimens). The bounding membranes appeared either fuzzy or were strongly defined (Fig. 5). Internally, most vesicles were electron-lucent, though wisps of electron-dense fibers were often present and in some cases the contents were of medium density or entirely electron-dense (Fig. 5C). The most electron-dense vesicles were 199–320 nm in size ($\bar{x}$ = 292 nm; SD = 44.6 nm; n = 15) and were not obviously restricted to the wart-like zones; they were also observed in other regions of the integument around the trunk (Fig. 5A). In between most electron-lucent vesicles was a ribosome-rich cytoplasm with occasional mitochondria, Golgi, and rER. Mitochondria were generally positioned close to the basal plasma membrane, but some were dispersed among vesicles and other times were present directly below the ICL. Some cytoplasmic regions below the ICL also contained regions of electron-dense cytoplasm, largely due to the abundance of ribosomes, but other organelles including potential autophagic bodies (Fig. 5D) were present and some organelles that could not always be identified.

Despite processing several individual females (from a single colony) in a partly contracted state, few animals showed evidence of exocytosis. Most vesicles remained within the swollen cytoplasm and only a few were in the process of exocytosis. These vesicles were fused to the ICL and created a pore with the apical plasma membrane (Fig. 5E and F). These vesicles were no more abundant in the ICL than vesicles in other regions of the integument, so it does not appear that preservation during contraction causes exocytosis. We cannot be certain that these fusion vesicles in the warts were actively exuding their contents or whether the observed vesicles were part of the natural process that characterizes the general rotifer integument (Koehler, 1965; 1966).

We processed a single specimen that had no vesicles in any warts (Fig. 6). This specimen was from a separate colony; only one colony member was sectioned and stained. The "empty" warts had a mostly electron-lucent cytoplasm devoid of ribosomes, with few mitochondria, an occasional nucleus within the wart body (only two warts were examined), and several membrane-bound vesicular bodies (Fig. 6A). These bodies were irregularly shaped (range: 149–267 nm; $\bar{x}$ = 214 nm, SD = 69 nm) and often had two or three laminae surrounding a clear or cloudy core (Fig. 6B). The membranes were often disrupted, and the core did not look similar to the cores present in the warts of the other specimens (compare to Fig. 4). Darkened patches of grainy cytoplasm were present around most vesicles.

4. Discussion

4.1. Rotifer defenses against predation

Rotifers are known to exhibit a variety of behavioral and morphological defenses (Gilbert, 2019; Parry et al., 2022; Wallace et al., 2015), but to date, no species has been shown definitively to secrete allomones that ward off predators. Colony formation, however, has been demonstrated to limit predation by making rotifers too large for gape-limited predators (Diéguez and Balseiro, 1998; Wallace, 1987). On the other hand, studies of the rotifer, *S. socialis*, have revealed this species to be unique because it appears to utilize both colony formation and allomones as forms of defense against invertebrate and vertebrate predators (Felix et al., 1995; Walsh et al., 2006). Adult females of *S. socialis* reside in colonies of 30–200 individuals and are permanently attached to a substrate such as an aquatic hydrophyte (Wallace, 1987). Colonial adults produce amictic (asexual) eggs, which they retain on a special structure called the oviferon. When embryos hatch, the larval females remain tethered to their parent by a glandular secretion emanating from their foot. However, egg hatching is synchronous so that larvae tend to leave the parent colony at the same time, but in doing so their tethers become entangled and eventually this connection breaks. The result is that hatched larvae remain connected, swim as a planktonic group before settling, and once settled, metamorphose and grow to adulthood on a new substratum; a process referred to as “geminative” colony formation (Wallace et al., 2015). Settled colonies are vulnerable to epiphytic predators that graze the substratum and so it is not unexpected that such rotifers would have behavioral and/or morphological defenses

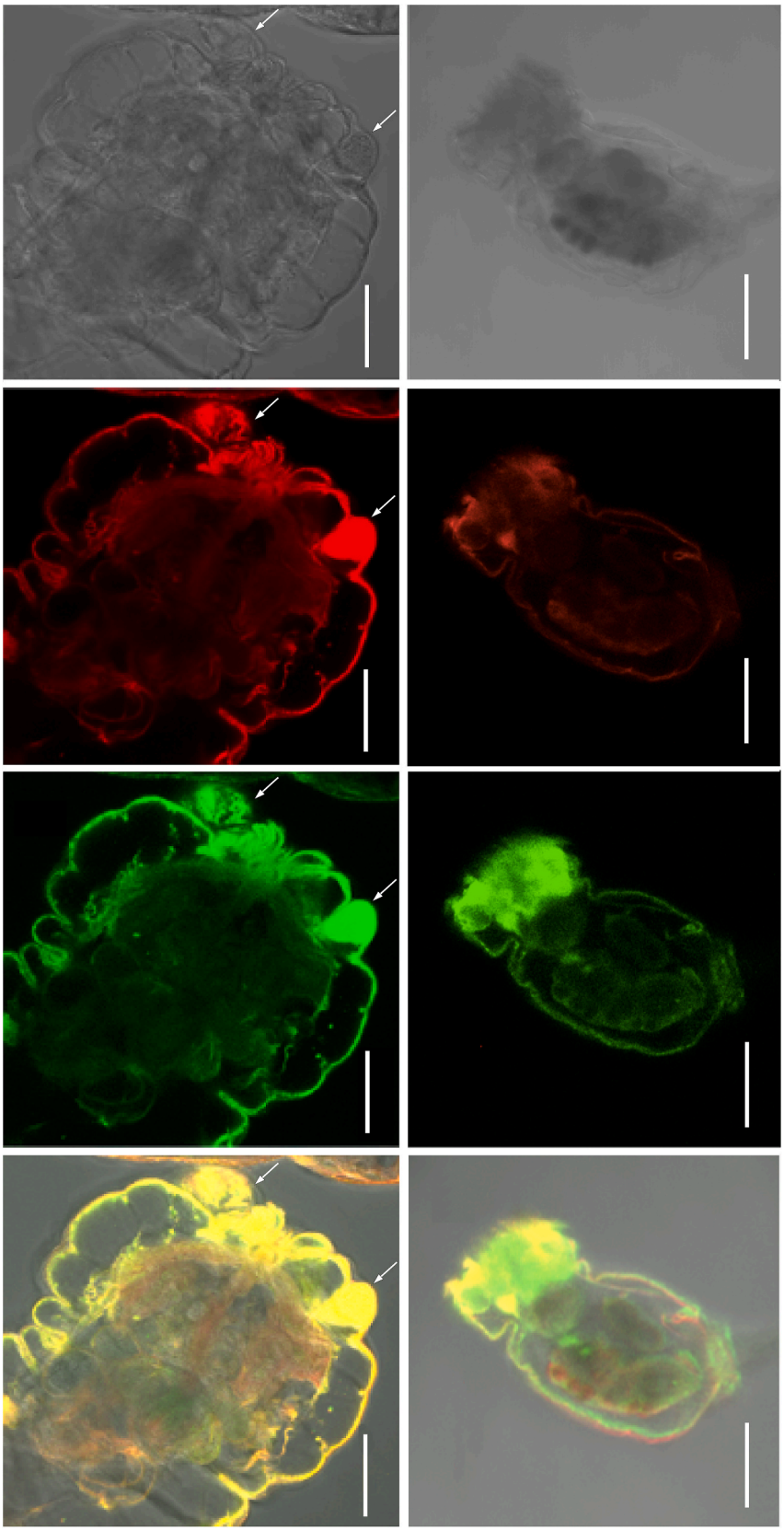

Fig. 2. Visualization of lipid probes in *Sinantherina socialis* (left) and *Epiphanes chihuahuaensis* (right). Top to bottom: specimens were photographed with brightfield microscopy, stained with Nile Red, stained for sphingomyelin (NBD-SM), and combined light and confocal images. Arrows indicate the location of warts in *S. socialis*. Scale bars: A-D = 50 μm; E-H, 100 μm.

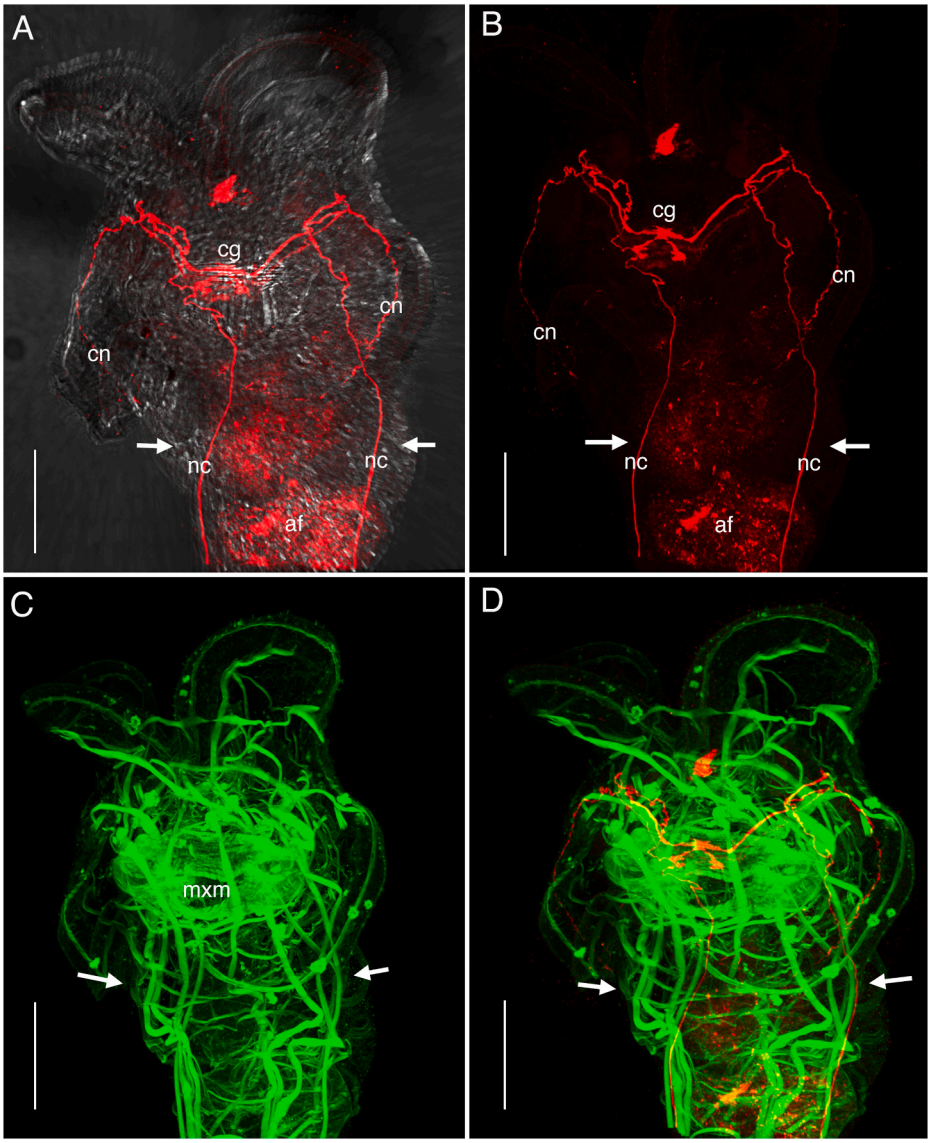

Fig. 3. Adult female *Sinantherina socialis* stained for serotonin (5-HT, red) and muscles (Alexa-488 phalloidin, green) and visualized with CLSM. Arrows indicate approximate location of the warts. A) Combined transmitted light and fluorescence image of anterior end; B) Fluorescence of serotoninergic neurites in the anterior end; C) Muscles in the anterior trunk region; D) Combined serotonin and phalloidin stains. Abbreviations: af, autofluorescence; cg, neurites of cerebral ganglion; cn, coronal neurites; mxm, muscles of the mastax; nc, nerve cords. Scales bars A–D: 20 μm.

against predation (Garcia, 2004). Researchers have hypothesized that the warts of *S. socialis*, and perhaps *S. semibullata*, function as deterrents against such predators through the secretion of allomones. Two predator-prey experiments appear to confirm that *S. socialis* is indeed unpalatable (Felix et al., 1995; Walsh et al., 2006). In the current study, we examine the ultrastructure of these wart-like bodies to determine whether they are in fact glandular, and if so, whether we can determine anything about the chemistries of potential allomones using cytochemical stains.

4.2. Do the warts of S. socialis function as exocrine glands?

Rotifer glands have not been well studied, but recent studies reveal that most glands, except for pedal glands that function in attachment, are syncytial (Yang and Hochberg, 2018; Yang et al., 2021). Rotifer glands appear to be restricted to specific areas within the syncytial integument, and in these regions are easily recognized by possessing a high abundance of synthetic machinery (e.g., ER, Golgi) and a high density of secretory vesicles or granules. For example, species of *Limnias* have trunk glands that are merely localized regions of the integument containing abundant organelles and secretions relative to the rest of the integument. These glands undergo regulative secretion, meaning they appear to store secretory vesicles for a period before exocytosis releases the gland contents through the apical plasma membrane and outside their bodies where a protective tube is built (Yang and Hochberg, 2018). In *S. socialis*, the warts are clearly glandular as they contain abundant organelles and numerous secretory vesicles within a defined region of the integument, similar to *Limnias*. Transmission electron microscopy reveals the warts of *S. socialis* to be independent, localized swellings of the integument without intracellular plasma membranes, i.e., they are part of the integumentary syncytium (Fig. 7). There is no obvious connection between the four warts other than through the continuum of the syncytial integument. Each wart is swollen relative to the integument around it: the swelling appears spindle-shaped with the center of the spindle filled with ribosome-rich cytoplasm, mitochondria, rER, and hundreds of membrane-bound secretion vesicles. A nucleus is usually present off center. Most secretion vesicles are oval to round, have electron-lucent cores, and range in size from 149 to 201 nm diameter ($\bar{x}$ = 175.5 nm ± 17.7 nm). Vesicles with electron-dense cores were occasionally present and measured on average 292 ± 44.6 nm; these vesicles were not unique to the swollen syncytium but were observed scattered across the integument. All wart-contained vesicles appeared destined for transport across the intracytoplasmic lamina (ICL), an intracellular, cuticle-like region that is positioned just below the plasma membrane of

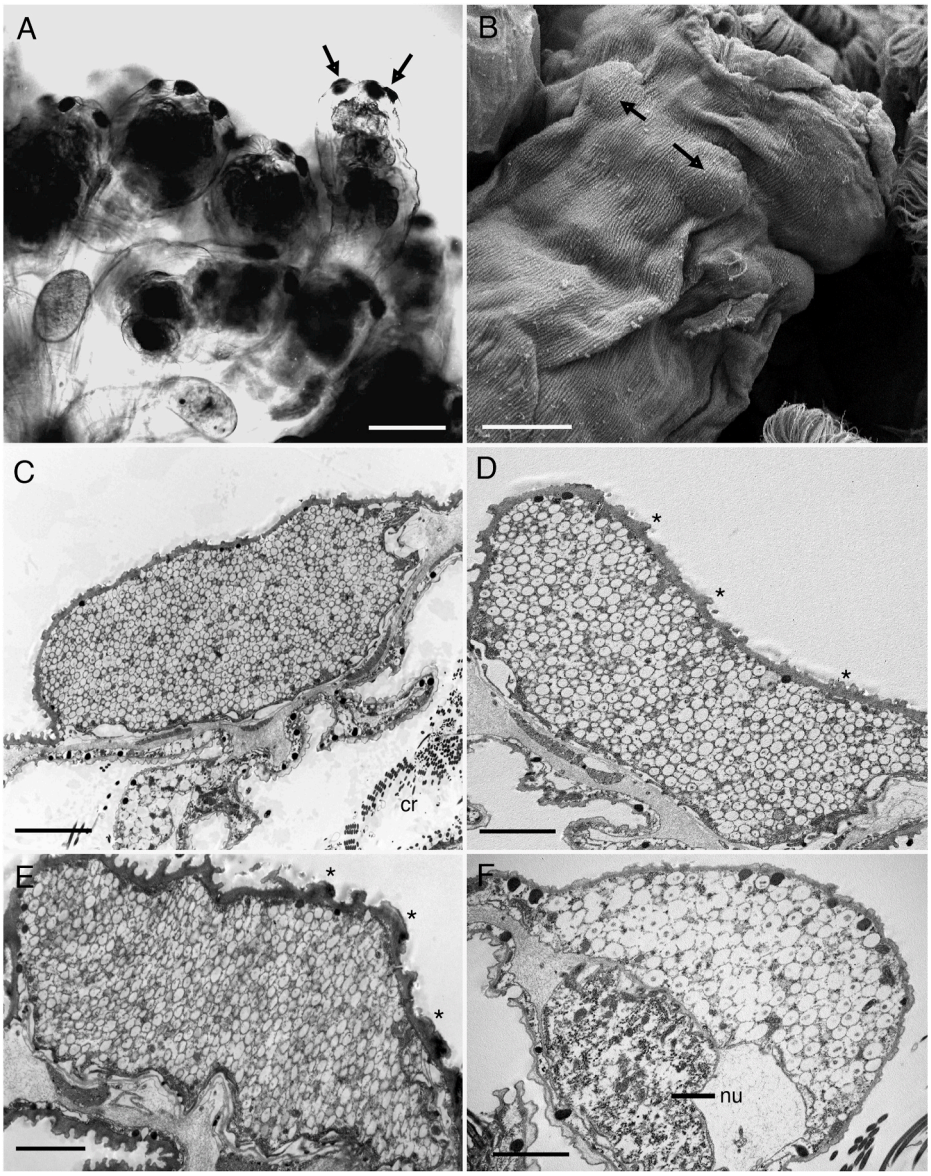

Fig. 4. Focus on the warts of *Sinantherina socialis*. A) Portion of a colony of retracted adult females under reflected light. Arrows point to warts (note the change in their appearance with a different lighting regime); B) Scanning electron microscopy of a single specimen (corona retracted) showing bulges (arrows) where two warts are located; C–F) Sections through all four warts of a single adult female. Asterisks indicate ridge-like patterns of the integument. Abbreviations: cr, corona; nu, nucleus Scale bars: A, 100 μm. B, 15 μm. C. 2 μm. D, 1.9 μm. E, 2.5 μm. F, 1.3 μm.

the integument. These vesicles appear to fuse individually with the ICL and release their contents en masse; this differs from the normal form of exocrine secretion in the rotifer integument where vesicles fuse with the plasma membrane one at a time (or at least not all at once) (Koehler, 1965; 1966; Yang et al., 2021). Vesicle fusion is probably followed by a recycling of the bounding membranes, which is characteristic of glands that undergo regulative secretion (De Camilli and Jahn, 1990; Kögel and Gerdes, 2009). Hence, there is no permanent pore to these glandular warts.

The behavior that probably leads to the synchronized expulsion of gland contents is longitudinal body contraction, which is observed when predators touch colony members (Felix et al., 1995). The glands are not enclosed in muscles nor directly innervated, which supports this hypothesis. However, this would also mean that each time a member contracts, regardless of the reason, secretions are exuded. Such a behavior would require continuous production of secretory vesicles, and so different members of a colony may therefore have different abundances of vesicles in their warts at any one time. We did not compare vesicle amounts between colony members, but observations suggest vesicle numbers appeared similar within individuals, i.e., all warts were either full or empty in a single specimen. Curiously, we have never observed increased evidence of exocytosis in contracted (preserved) specimens, so there must be other factors that lead to simultaneous expulsion of the secretion products. Interestingly, we did process a single contracted specimen from a separate colony that had "empty" warts. These warts were of a similar size and shape to warts filled with secretions in other individuals, but the cytoplasm lacked the secretion vesicles present in other specimens (compare Figs. 4 and 6), and the cytoplasm was virtually devoid of free ribosomes. Instead, it contained an abundance of vesicle-shaped bodies, some with electron-lucent cores, and others with disrupted membranes that were peeling inward to the core or externally unraveling (see Fig. 6B). Whether these bodies represent empty secretion vesicle membranes is unknown, but if they are, then their appearance suggests that the secretion vesicles have multiple membranes, which to our knowledge would be unusual. The specimen with "empty" warts did not have any obviously secreted contents on the outside of the integument, nor did we observe any other specimens (live specimens with light microscopy or preserved specimens with scanning electron microscopy) that showed evidence of exuded secretory material. Of course, clear gland contents would be difficult to detect *in situ* and the secretions may rinse off or dissolve during preparation for EM.

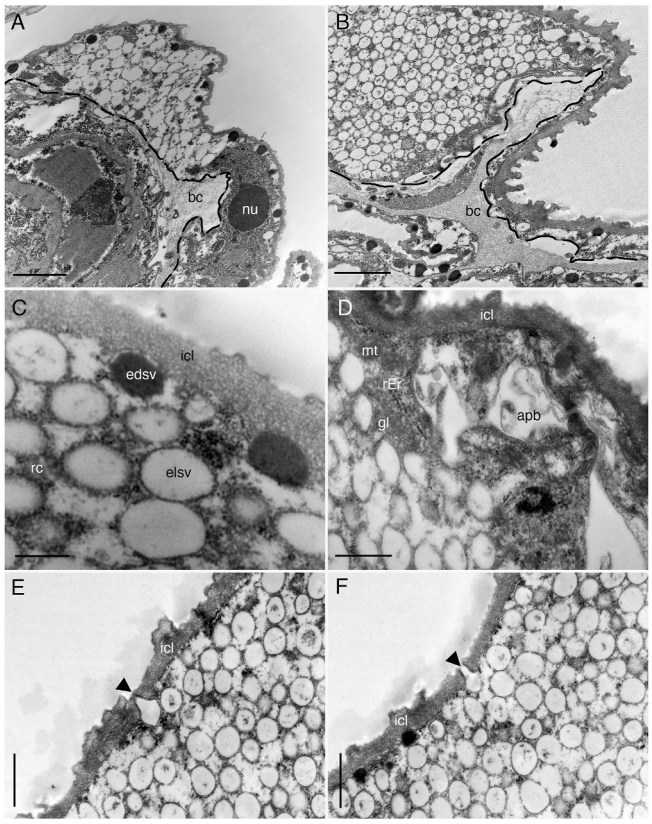

Fig. 5. Transmission electron micrograph of ultrastructure of the warts of a single female of *Sinantherina socialis*. A) Longitudinal section through a wart on the dorsolateral body surface. Black line outlines the basal plasma membrane that differentiates the integument from the blastocoel and other underlying organ systems; B) Closeup of a different wart on the same specimen. Black line demarcates base of integument; C) Closeup of secretion vesicles that reside in the ribosome-rich cytoplasm below the intracytoplasmic lamina (ICL) of the integument; D) Closeup of a wart showing other organelles in the cytoplasm of a wart. Most organelles were pushed to the periphery of the wart due to the abundance of secretion vesicles; E) Closeup of the intracytoplasmic lamina showing the fusion of a vesicle (arrowhead) to create a bulb-like shape; F) Closeup of the intracytoplasmic lamina revealing the opening of a secretion vesicle (arrowhead) after fusion with the intracytoplasmic lamina. Abbreviations: apb autophagic body; bc, body cavity; edsv, electron dense secretion vesicle; elsv, electron-lucent secretion vesicle; gl, Golgi membranes; icl, intracytplasmic lamina of the integument; mt, mitochondria; nu, nucleus; rER, rough endoplasmic reticulum; rc, ribosome rich cytoplasm. Scale bars A, 2 μm. B, 1.2 μm. C, 300 nm. D, 500 nm. E, 700 nm. F, 700 nm.

4.3. Do the warts contain compounds that function for defense?

We attempted two generic methods to characterize wart contents: 1) fluorescent probes in whole mount specimens, and 2) standard TEM fixatives and heavy metal stains. We used two fluorescent stains to determine whether proteins or neutral lipids were present in the warts. LavaCell revealed the presence of primary amines in the warts, but the fluorescence was no different from the rest of the body. Nile Red was used for neutral lipids and showed intense fluorescence in the warts relative to the rest of the body. Unfortunately, the intensity of the staining made resolution inside of the warts difficult to determine, so we are unsure where the neutral lipids are located specifically within the wart bodies. Importantly, Nile Red is also known to fluoresce in the presence of proteins with hydrophobic domains (Greenspan et al., 1985), so we are hesitant to classify the secretory contents as strictly of neutral lipid origin. Of the remaining probes, only phosphatidylinositol (PI) and sphingomyelin (SM) showed intense fluorescence in the warts. Both of these compounds are important components of cell membranes (Futerman, 2016), so their presence in the warts is not unusual. While PI and its phosphorylated derivatives (e.g., PIP, PIP2) are involved in cell signaling (Hernandez et al., 2007), SM and other sphingolipids are found in lipid rafts. Lipid rafts participate in various cellular processes including cell–cell communications, receptor internalization, and receptor signaling (De Chatterjee et al., 2015). Our reasoning behind their use was to determine, prior to TEM, whether the warts contained abundant membrane-bound secretion vesicles that might hint at the warts' function as exocrine glands. Once determined, we applied TEM to achieve higher resolution.

While the warts are obviously pigmented (white or brown) when animals are visualized with different forms of light microscopy, their contents are largely translucent when visualized with TEM. Osmium preservation did not darken the wart contents (in whole mount or sectioned material), and when combined with uranyl acetate and lead citrate stains, the warts' contents remained electron-lucent. We do not know what happens to the pigment (visualized under light microscopy) after preservation and embedding, and we cannot be certain that the pigment is not what makes the rotifer unpalatable. With this in mind, we acknowledge the possibility that the transparency of the secretion vesicles in the warts after embedding may be an artifact of our methods, i.e., the unpalatable compounds were lost during preparation. However, the contents of other secretion vesicles in the integument remained intact and heavily stained, so we think the electron-lucent nature is natural to the warts.

If the warts are indeed the source of unpalatable allomones, as behavioral analyses would suggest, then their contents may in fact be saturated fatty acids based on our staining profiles. Nile Red staining would seem to indicate presence of saturated lipids in the warts, and the absence of heavy metal deposition in the secretory vesicles would seem to rule out unsaturated lipids and phenolic compounds (normally stained with OsO_4; Nelson and Griffith (1977)), nucleic acids, or–NH2 and –COOH groups (stained with uranyl acetate (Lombardi et al., 1971);). Saturated fatty acids such as lactones are volatile compounds synthesized naturally by bacteria, yeast, and plants (Silva et al., 2021) where they can function as attractants and repellants (Chadwick et al., 2013). They are also well known to have strong aromatic and palatable qualities, which makes their synthesis useful for human perfumes and foods (Labuda, 2009). It is appealing to think the secretory vesicles of *S. socialis* are lactone-filled compounds with similar aromatic qualities, but proof will require much more detailed characterization.

4.4. Future directions for gland analysis and function

The next steps in the characterization process for the wart-like glands can come in many forms. There are still several generic methods for detecting proteins, carbohydrates, and lipids in animals prepared for brightfield microscopy (Presnell and Schreibman, 1997), but these methods may not achieve the necessary resolution because of the size of the warts. CLSM may help to increase resolution when combined with cytochemical and immunocytochemical stains (Stockert and Blázquez-Castro, 2017), but these may still be limited in their specificity. Electron microscopy may achieve the highest resolution, and while there are several stains that can provide excellent insights (Angermüller and Fahimi, 1982; Macrae and Meetz, 1970; Thiery, 1967), they can still only get at a broad classification of potential chemicals and therefore will lead to an unsatisfactory understanding of the unpalatability (potentially lactone-based) factor(s).

In his review of the chemical ecology of rotifers, Snell (1998) discussed several modern methods of fractionation that can be employed to achieve a better understanding of rotifer secretions. He posits that bioassay-guided techniques will help elucidate the functions of secretions (e.g., allomones, kairomones, pheromones, etc.), and that such techniques are applicable to even the smallest animals such as rotifers. More contemporary studies have used transcriptome- and genome-wide screening to search for specific secretions, such as lectins (Gerdol, 2022),

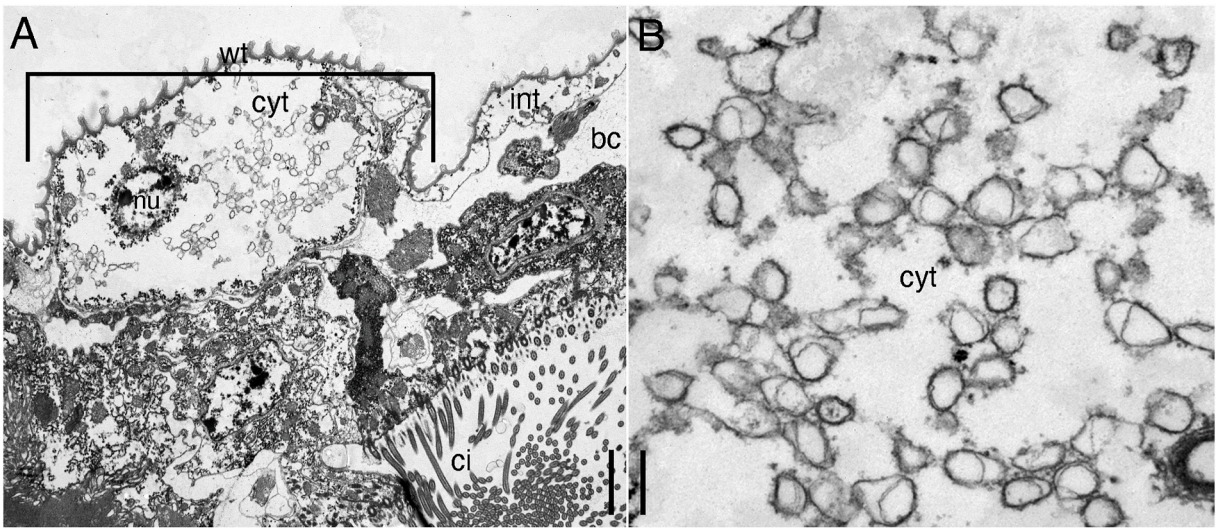

Fig. 6. Transmission electron micrograph of a single wart of an adult female *Sinantherina socialis* that appears empty of secretion vesicles. A) The wart contains a single nucleus and electron-lucent cytoplasm with few mitochondria and some membranes. The apical plasma membrane forms numerous ridge-like ornamentations; B) Closeup of the same wart as in A, but with a focus on the oval membranes in the wart cytoplasm. Abbreviations: bc, body cavity; ci, cilia of retracted corona; cyt, cytoplasm of wart; int, syncytial integument; nu, nucleus; wt, wart. Scale bars: A, 1.5 μm. B. 225 μm.

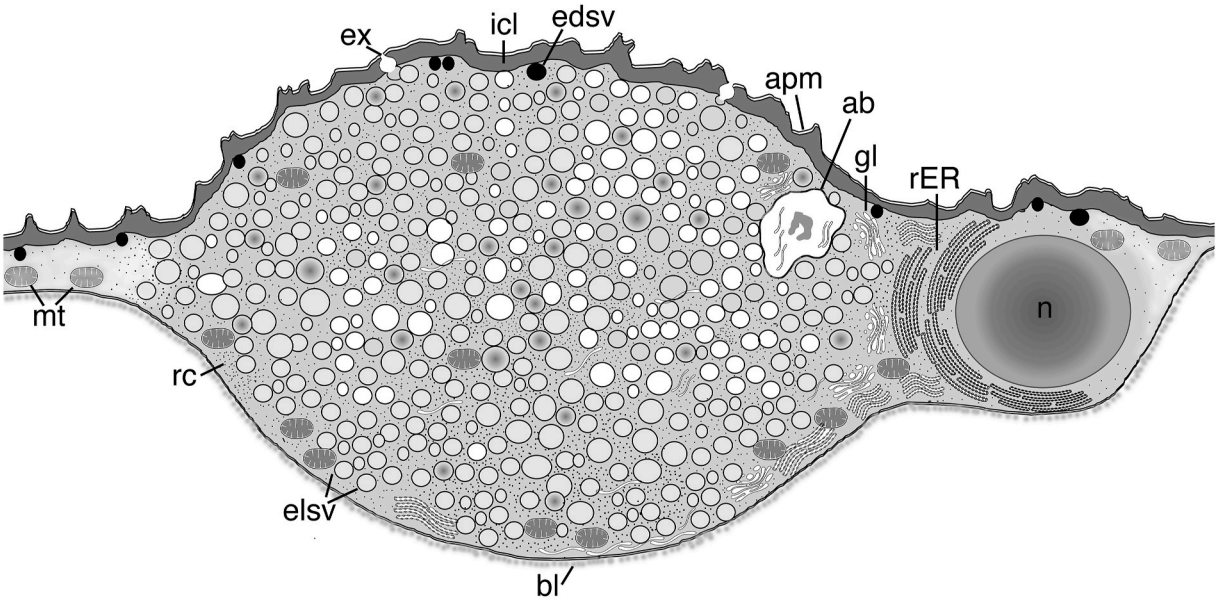

Fig. 7. Schematic of a wart of female *Sinantherina socialis*. The wart is acellular (a localized expansion of the integumental syncytium) and generally contains a single peripheral nucleus, abundant secretion vesicles, and various other organelles distributed within and around the periphery of the wart. Abbreviations: ab, autophagic body; apm, apical plasma membrane; bl, basal lamina; elsv, electron-lucent secretion vesicle; edsv, electron dense secretion vesicle; ex, external pore created by fusion of a secretion vesicle with the plasma membrane; icl; icl, intracytoplasmic lamina; gl, Golgi; mt, mitochondria; n, nucleus; rc, ribosome-rich cytoplasm; rER, rough endoplasmic reticulum.

but to date, the genomes of rotifers suspected to secrete allomones have not been published. Recently, we have sequenced the genome of *S. socialis*, but the annotation is still in progress. Future studies on the chemistry of *S. socialis* allomones may therefore benefit from similar modern approaches if biosynthetic pathways of lactone production can be targeted through transcriptomic and genomic methodologies.

Declaration of competing interest

The authors declare that they have no known competing financial interests or personal relationships that could have appeared to influence the work reported in this paper.

Data availability

Data will be made available on request.

Acknowledgements

Collections in Big Bend National Park were conducted under permit BIBE-2001-SCI-0058; we thank R. Skiles for his help in securing permission to work in the park. Collections in Hueco Tanks State Historic Site were conducted under permit 07–02. Rotifers from Hawaii were collected under permit to T. Schröder. We thank Dr. Joanne T. Ellzey and Marian Viveros for their help in the Analytical Cytology Core

Facility (National Institutes of Health, 5G12 RR08124-09). This project was funded in part by several agencies: Bridges to the Futures Program; (National Institutes of Health GMS-5R25GM49011-05); the National Science Foundation, DEB 2051704 and DEB 1257068 (E J. Walsh); the National Science Foundation DEB 1257116 and 2051710 (R L. Wallace), and National Science Foundation DEB 2051684 (R. Hochberg). Technical help was provided by core research facilities at UTEP funded by National Institutes of Health 5G12RR08124. The content is solely the responsibility of the authors and does not necessarily represent the official views of the National Institutes of Health or the National Science Foundation. We thank the Ripon College professional librarians for their help in securing some of the works that we cite in this paper. We also thank the staff at the Electron Microscopy Facility at the UMASS Chan Medical School in Worcester, MA for their assistance.

Appendix A. Supplementary data

Supplementary data to this article can be found online at https://doi.org/10.1016/j.jcz.2023.03.001.

References

Allen, R.L., Wallace, R.L., Sisson, B.E., 2016. A rotifer based technique to rear zebrafish larvae in small academic settings. Zebrafish 13, 281–286.
Almeda, R., van Someren Gréve, H., Kiørboe, T., 2017. Behavior is a major determinant of predation risk in zooplankton. Ecosphere 8, e01668.
Angermüller, S., Fahimi, H.D., 1982. Imidazole-buffered osmium tetroxide: an excellent stain for visualization of lipids in transmission electron microscopy. Histochem. J. 14, 823–835.
Balsamo, M., Artois, T., Smith, J.P., Todaro, M.A., Guidi, L., Leander, B.S., Van Steenkiste, N.W., 2020. The curious and neglected soft-bodied meiofauna: Rouphozoa (Gastrotricha and Platyhelminthes). Hydrobiologia 847, 2613–2644.
Buonanno, F., Anesi, A., Di Giuseppe, G., Guella, G., Ortenzi, C., 2017. Chemical defense by erythrolactones in the euryhaline ciliated protist, *Pseudokeronopsis erythrina*. Zool. Sci. 34, 42–51.
Buonanno, F., Catalani, E., Cervia, D., Cimarelli, C., Marcantoni, E., Ortenzi, C., 2020. Natural function and structural modification of climacostol, a ciliate secondary metabolite. Microorganisms 8, 809.
Buonanno, F., Harumoto, T., Ortenzi, C., 2013. The defensive function of trichocysts in *Paramecium tetraurelia* against metazoan predators compared with the chemical defense of two species of toxin-containing ciliates. Zool. Sci. 30, 255–261.
Buskey, E.J., Strickler, J.R., Bradley, C.J., Hartline, D.K., Lenz, P.H., 2017. Escapes in copepods: comparison between myelinate and amyelinate species. J. Exp. Biol. 220, 754–758.
Carman, K.R., Thistle, D., Ertman, S.C., Foy, M., 1991. Nile red as a probe for lipid-storage products in benthic copepods. Mar. Ecol. Prog. Ser. 74, 307–311.
Chadwick, M., Trewin, H., Gawthrop, F., Wagstaff, C., 2013. Sesquiterpenoids lactones: benefits to plants and people. Int. J. Mol. Sci. 14, 12780–12805.
De Camilli, P., Jahn, R., 1990. Pathways to regulated exocytosis in neurons. Annu. Rev. Physiol. 52, 625–645.
De Chatterjee, A., Mendez, T.L., Roychowdhury, S., Das, S., 2015. The assembly of GM1 glycolipid- and cholesterol-enriched raft-like membrane microdomains is important for giardial encystation. Infect. Immun. 83, 2030–2042.
Diéguez, M., Balseiro, E., 1998. Colony size in *Conochilus hippocrepis*: defensive adaptation to predator size. Hydrobiologia 387/388, 421–425.
Ehrenberg, C., 1830. Organisation, Systematik und geographisches Verhältnifs der Infusionsthierchen. Dümmler, F., Berlin, p. 108.
Felix, A., Stevens, M.E., Wallace, R.L., 1995. Unpalatability of a colonial rotifer, *Sinantherina socialis*, to small zooplanktivorous fishes. Invertebr. Biol. 114, 139–144.
Fontaneto, D., De Smet, W.H., Melone, G., 2008. Identification key to the genera of marine rotifers worldwide. Meiofauna Marina 16, 75–99.
Fontaneto, D., De Smet, W.H., Ricci, C., 2006. Rotifers in saltwater environments, re-evaluation of an inconspicuous taxon. J. Mar. Biol. Assoc. U. K. 86, 623–656.
Fradkin, S.C., 2001. Rotifer distributions in the coastal waters of the northeast Pacific Ocean. Hydrobiologia 466/467, 173–177.
Futerman, A.H., 2016. Sphingolipids. In: Ridgway, N.D., McLeod, R.S. (Eds.), Biochemistry of Lipids, Lipoproteins and Membranes, sixth ed. Elsevier, Amsterdam, pp. 297–326.
Garcia, M.A., 2004. The Asexual Life History of the Colonial Rotifer, *Sinantherina socialis* (Linnaeus). Ph.D. dissertation submitted in partial fulfillment of the degree Doctor of Philosophy. Department of Biology and Evolutionary Biology. Yale University, New Haven, CT, p. 129. New Haven, p. 129 pp. (UMI Number: 3125197).
Gerdol, M., 2022. First insights into the repertoire of secretory lectins in rotifers. Mar. Drugs 20, 130.
Gilbert, J.J., 1980. Observations on the susceptibility of some protists and rotifers to predation by *Asplanchna girodi*. Hydrobiologia 73, 87–91.
Gilbert, J.J., 2019. Attachment behavior in the rotifer *Brachionus rubens*: induction by *Asplanchna* and effect on sexual reproduction. Hydrobiologia 844, 9–20.
Greenspan, P., Mayer, E.P., Fowler, S.D., 1985. Nile red: a selective fluorescent stain for intracellular lipid droplets. JCB (J. Cell Biol.) 100, 965–973.
Hampton, S.E., Gilbert, J.J., 2001. Observations of insect predation on rotifers. Hydrobiologia 446/447, 115–121.
Hernandez, Y., Zamora, G., Ray, S., Chapoy, J., Chavez, E., Valvarde, R., Williams, E., Aley, S.B., Das, S., 2007. Transcriptional analysis of three major putative phosphatidylinositol kinase genes in a parasitic protozoan, *Giardia lamblia*. J. Eukaryot. Microbiol. 54, 29–32.
Hershey, A.E., Dodson, S.I., 1987. Predator avoidance by *Cricotopus*: cyclomorphosis and the importance of being big and hairy. Ecology 68, 913–920.
Herzog, Q., Tittgen, C., Laforsch, C., 2016. Predator-specific reversibility of morphological defenses in *Daphnia barbata*. J. Plankton Res. 38, 771–780.
Hochberg, R., Hochberg, A., Chan, C., 2015. Ultrastructure of the rotifer integument: peculiarities of *Sinantherina socialis* (Monogononta: Gnesiotrocha). Invertebr. Biol. 134, 181–188.
Hochberg, R., Lilley, G.W., 2010. Neuromuscular organization of the freshwater colonial rotifer, *Sinantherina socialis*, and its implications for understanding the evolution of coloniality in Rotifera. Zoomorphology 129, 153–162.
Kerfoot, W.C., 1982. A question of taste: crypsis and warning coloration in freshwater zooplankton communities. Ecology 63, 538–554.
Kerfoot, W.C., Kellogg, D.L.J., Strickler, J.R., 1980. Visual observations of live zooplankters: evasion, escape, and chemical defenses. In: Kerfoot, W.C. (Ed.), Evolution and Ecology of Zooplankton Communities. The University Press of New England, Hanover, NH, pp. 10–27.
Koehler, J.K., 1965. A fine-structure study of the rotifer integument. J. Ultra. Res. 12, 113–134.
Koehler, J.K., 1966. Some comparative fine structure relationships of the rotifer integument. J. Exp. Zool. 162, 231–244.
Kögel, T., Gerdes, H.H., 2009. Maturation of secretory granules. In: Rehfeld, J., Bundgaard, J. (Eds.), Cellular Peptide Hormone Synthesis and Secretory Pathways. Results and Problems in Cell Differentiation. Springer, Berlin, pp. 137–184.
Lambl, W., 1859. Mikroskopische untersuchungen der Darmexcrete. Vierteljahrsschr. Prakst. Heikunde (Prague) 61, 1–58.
Labuda, I., 2009. Flavor compounds. In: Schaechter, M. (Ed.), Encyclopedia of Microbiology, third ed. Elsevier, Amsterdam, pp. 305–320.
Linnaeus, C., 1758. Systema Naturæ Per Regna Tria Naturæ, Secundum Classes, Ordines, Genera, Species, Cum Characteribus, Differentiis, Synonymis, Locis. Tomus I. Editio Decima, Reformata. Laurentii Salvii, Stockholm. pp. 823.
Lombardi, L., Prenna, G., Okolicsanyi, L., Gautier, A., 1971. Electron staining with uranyl acetate. Possible role of free amino groups. J. Histochem. Cytochem. 19, 161–168.
Lubzens, E., Tandler, A., Minkoff, G., 1989. Rotifers as food in aquaculture. Hydrobiologia 186/187, 387–400.
Macrae, E.K., Meetz, G.D., 1970. Electron microscopy of ammoniacal silver reaction for histones in erythropoietic cells of chick. JCB (J. Cell Biol.) 45, 235–245.
Nelson, A.J., Griffith, W.P., 1977. Tissue fixation and staining with osmium tetroxide: the role of phenolic compounds. J. Histochem. Cytochem. 26, 138–140.
Parry, V., Schlägel, U.E., Tiedemann, R., Weithoff, G., 2022. Behavioural responses of defended and undefended prey to their predator—a case study of Rotifera. Biology 11, 1217.
Presnell, J.K., Schreibman, M.P., 1997. Humanson's Animal Tissue Techniques. The Johns Hopkins University Press, Baltimore.
Schneider, C.A., Rasband, W.S., Eliceiri, K.W., 2012. NIH Image to ImageJ: 25 years of image analysis. Nat. Methods 9, 671–675.
Schröder, T., Walsh, E.J., 2007. Cryptic speciation in the cosmopolitan *Epiphanes senta* complex (Monogononta, Rotifera) with the description of new species. Hydrobiologia 593, 129–140.
Silva, R., Coelho, E., Aguiar, T.Q., Domingues, L., 2021. Microbial biosynthesis of lactones: gaps and opportunities towards sustainable production. Appl. Sci. 11, 8500.
Snell, T.W., 1998. Chemical ecology of rotifers. Hydrobiologia 387/388, 267–276.
Snell, T.W., Johnston, R.K., Matthews, A.B., 2018. Utilizing *Brachionus* biodiversity in marine finfish larviculture. Hydrobiologia 844, 149–162.
Sonda, S., Štefanić, S., Hehl, A.B., 2008. A sphingolipid inhibitor induces a cytokinesis arrest and blocks stage differentiation in *Giardia lamblia*. Antimicrob. Agents Chemother. 52, 563–569.
Stenson, J.A.E., 1987. Variation in capsule size of *Holopedium gibberum* (Zaddach): a response to invertebrate predation. Ecology 68, 928–934.
Stevens, T.L., Gibson, G.R., Adam, R.D., Maier, J., Allison-Ennis, M., S, D, 1997. Uptake and cellular localization of exogenous lipids by *Giardia lamblia*, a primitive eukaryote. Exp. Parasitol. 86, 133–143.
Stockert, J.C., Blázquez-Castro, A., 2017. Fluorescence Microscopy in the Life Sciences. Bentham Science Publishers, Sharjah, UAE.
Thiery, J.P., 1967. Mise em evidence des polysaccharides sur coupes fines en microscopie electronique. J. Microsc. 6, 987–1018.
Thorpe, V.G., 1889. IX.—Description of a new species of *Megalotrocha*. Journal of the Royal Microscopical Society, pp. 613–616.
Thorpe, V.G., 1893. The Rotifera of China. J. R. Microsc. Soc. 13, 145–152.
Wallace, R.L., 1987. Coloniality in the phylum Rotifera. Hydrobiologia 147, 141–155.
Wallace, R.L., Snell, T.W., Ricci, C., Nogrady, T., 2006. Rotifera. Volume 1: Biology, Ecology and Systematics, second ed. Backhuys Publishers, Leiden.
Wallace, R.L., Snell, T.W., Smith, H.A., 2015. Phylum Rotifera. In: Thorp, J.H., Rogers, D. C. (Eds.), Thorp and Covich's Freshwater Invertebrates. Elsevier, Waltham, MA, pp. 225–271.
Walsh, E.J., Salazar, M., Remirez, J., Moldes, O., Wallace, R.L., 2006. Predation by invertebrate predators on the colonial rotifer *Sinantherina socialis*. Invertebr. Biol. 125, 325–335.

Walsh, E.J., Schröder, T., Wallace, R.L., Ríos Arana, J.V., Rico-Martínez, R., 2008. Rotifers from selected inland saline waters in the Chihuahuan Desert of México. Saline Syst. 4, 7.
Walsh, E.J., Smith, H.A., Wallace, R.L., 2014. Rotifers of temporary waters. Int. Rev. Hydrobiol. 99, 3–19.
Yang, H., Hochberg, R., 2018. Ultrastructure of the extracorporeal tube and "cement glands" in the sessile rotifer *Limnias melicerta* (Rotifera: Gnesiotrocha). Zoomorphology 137, 1–12.
Yang, H., Hochberg, R., Walsh, E.J., Wallace, R.L., 2021. Ultrastructure of the extracorporeal secretions of four sessile species of Rotifera (Gnesiotrocha) with observations on the chemistry of the gelatinous tube. Invertebr. Biol. 140, e12318.